Spatial and temporal divergence of the torquatus species group of the subterranean rodent *Ctenomys*

D. A. Caraballo[1,2,3], M. S. Rossi[1,2]

[1] *Universidad de Buenos Aires, Facultad de Ciencias Exactas y Naturales, Buenos Aires, Argentina.*
[2] *CONICET-Universidad de Buenos Aires, Instituto de Fisiología, Biología Molecular y Neurociencias (IFIBYNE), Buenos Aires, Argentina.*
[3] *E-mail: dcaraballo@fbmc.fcen.uba.ar*

Abstract

Subterranean rodents of the genus *Ctenomys* have experienced an explosive radiation and rapidly colonized the southern cone of South America. The torquatus group, one of the main groups of the genus, comprises several species and species complexes which inhabit the eastern part of the distribution of *Ctenomys* including southern Brazil, northern and central Uruguay and north-eastern Argentina. This group has undergone a high chromosomal diversification with diploid numbers varying from 41 to 70. The aim of this study was to investigate the origins of the torquatus group as well as its diversification patterns in relation to geography and cladogenesis. Based on mitochondrial cytochrome b nucleotide sequences we conducted a Bayesian multi-calibrated relaxed clock analysis to estimate the ages of the torquatus group and its main lineages. Using the estimated evolutionary rate we performed a continuous phylogeographic analysis, using a relaxed random walk model to reconstruct the geographic diffusion of the torquatus group in a temporal frame. The torquatus group originated during the early Pleistocene between 1.25 and 2.32 million years from the present in a region that includes the northwest of Uruguay and the southeast of the Brazilian state of Río Grande do Sul. Most lineages have dispersed early towards their present distribution areas going through subsequent range expansions in the last 800,000 – 700,000 years. *Ctenomys torquatus* went through a rapid range expansion for the last 200,000 years, becoming the most widespread species of the group. The colonization of the Corrientes and Entre Ríos Argentinean provinces supposes at least two crossing events across the Uruguay River between 1.0 and 0.5 million years before the present, in the context of a cold and dry paleoenvironment. The resulting temporal and geographic frame enables the comprehension of the incidence of both, the amplitude of distribution areas and divergence times into the patterns of chromosomal diversification found in the group.

Contents

Introduction

Temporal and spatial frameworks are crucial to acquire a comprehensive scenario of species evolution. Theory and methods for estimating phylogenetic divergence times and connecting historical processes in evolution with spatial distributions have undergone profound changes during the last decade. Bayesian Markov Chain Monte Carlo (MCMC) methods offer a statistical framework to estimate parameters combining the information provided by the data with prior knowledge supplied by the researcher, integrating simultaneously many models over parameter uncertainty (Drummond and Rambaut, 2007). Phylogenies and divergence times can be estimated in the face of uncertainty in evolutionary rates and calibration times (Drummond et al., 2006). In molecular dating analysis the number of calibrated nodes, their relative position and the way in which uncertainty is modelled could be determinant issues in resulting estimations (Ho and Phillips, 2009 and references therein). In this sense, it is well accepted that

relying on as many calibrated nodes as possible is ideal to obtain accurately estimated divergence times (Hug and Roger, 2007; Ho and Phillips, 2009; Lukoschek et al., 2012; Bibi, 2013; Soares and Schrago, 2015). Bayesian MCMC methods also enable the simultaneous reconstruction of evolutionary and geographic history, accounting for phylogenetic, demographic and geographic uncertainty, under stochastic process-driven models that accommodate spatial diffusion in discrete and continuous space (Bloomquist et al., 2010; Lemey et al., 2009, 2010). Geographic origins and dispersal patterns of influenza and rabies viruses (Lemey et al., 2009) but also of modern polar bears (Edwards et al., 2011) as well as of the *Agama agama* species group of African lizards (Leaché et al., 2016) have been studied employing this approach.

Based on complete cytochrome b (cyt-b) gene sequences, in this study we made use of both approaches to get a more comprehensive scenario of the divergence process of a group of South American subterranean rodents of the genus *Ctenomys* (tuco-tucos) known as the torquatus group. The torquatus group which inhabits the eastern part of the distribution of the genus comprises at least 12 independent lineages, 8 out of this were described integrally from morphological, chromosomal and genetic points of view, as species. *Ctenomys torquatus* Lichtenstein, 1830, has the widest geographic range in the group, encompassing an area that spans from the southern half of the state of Río Grande do Sul in Brazil to the northern half of Uruguay (Freitas, 1995; Fernandes et al., 2009). *Ctenomys lami* Freitas, 2001, and *C. minutus* Nehring 1887, two closely related species, inhabit sandy fields and dunes in the south-eastern Brazilian coastal plains (Lopes et al., 2013). *Ctenomys ibicuiensis* Freitas, Fernandes, Fornel and Roratto, 2012 has a restricted geographic distribution in southern Brazil (Freitas et al., 2012). The *C. pearsoni* Lessa and Langguth, 1983 complex is distributed along the Uruguayan Atlantic coast (Tomasco and Lessa, 2007) and in the Argentinean Entre Ríos province (Caraballo et al., 2016). The three species *C. roigi* Contreras, 1988, *C. dorbignyi* Contreras and Contreras, 1984 and *C. perrensi* Thomas, 1896, plus four lineages that conform the Corrientes group are distributed in the homonym Argentinean province (Caraballo and Rossi, 2017 and references therein) (Figure 1A).

Divergence times of the major lineages that comprise the speciose genus *Ctenomys*, have been estimated by Parada and collaborators (2011) on the basis of cyt-b sequences. However, the torquatus group was not completely represented in this study and, with

the exception of *C. torquatus*, whose age has been recently estimated (Roratto et al., 2015), the origin of the main lineages of this highly diverse group has not been dated.

The genus *Ctenomys* is one of the most chromosomally variable mammals, with diploid numbers (2n) ranging from 10 to 70, and as such, they constitute a model for studying speciation and chromosomal evolution (Cook et al., 1990; Ortells et al., 1990; Reig et al., 1990). Chromosomal variability in the torquatus group includes polymorphisms and polytypisms. Diploid numbers range from 40 to 46 in *C. torquatus* (Fernandes et al., 2009), from 42 to 58 in *C. lami* plus *C. minutus* (Freitas, 2007; Lopes et al., 2013), from 56 to 70 in the case of *C. pearsoni* complex (Tomasco and Lessa, 2007, and references therein) and from 41 to 70 in the Corrientes group (Caraballo et al., 2015 and references therein). *Ctenomys ibicuiensis* depicts a unique karyotype with 2n = 50 (Freitas et al., 2012). Studying these lineages within a temporal frame allows inferring the rates of chromosomal change and assessing if karyotypic dynamics show a stable pattern or has experienced accelerations/decelerations along the evolution of this chromosomally diverse group.

The objective of this study was to reconstruct the geographic diffusion of the torquatus group along its evolution. To achieve this goal, we estimated the age of the torquatus group and its main lineages under a Bayesian multi-calibrated relaxed clock analysis. Based on the estimated clock rate, we conducted a Bayesian continuous phylogeographic analysis, using a relaxed random walk model (Lemey et al., 2010). The patterns of chromosomal diversification, as well as the strength of the large Uruguay River as a barrier to dispersal, were discussed under the light of the resulting spatio-temporal frame.

Material and methods

Overall methodology

We conducted a multi-calibrated analysis based on cyt-b sequences from 43 Octodontoidea and 89 *Ctenomys* representatives available in GenBank. This analysis enabled the age estimation of the torquatus group most recent common ancestor (MRCA) as well as divergence times of the main lineages within the group. The estimated clock rate (and its uncertainty) was used as a prior in a subsequent Bayesian phylogeographical analysis employing a broader
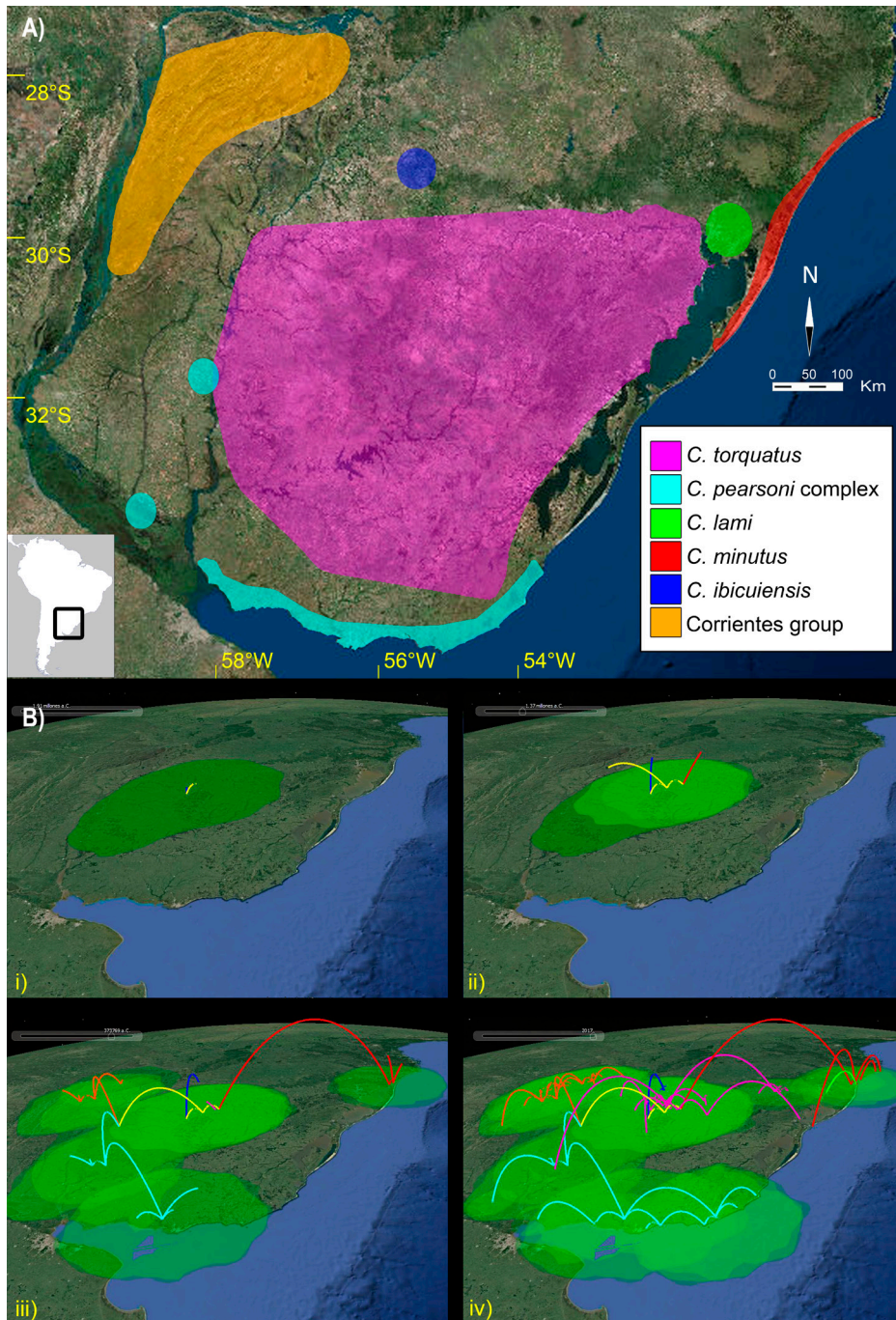
Figure 1A. Species ranges of the torquatus group. The extents of occurrence were retrieved from The IUCN Red List of Threatened Species (www.iucnredlist.org). In the case of *C. pearsoni*, the Entrerrianan disjunct populations were added, while in the Corrientes group the colored area reflects the extent of occurrence of all populations of the group (without species distinction). *B*. Spatio-temporal dynamics of the torquatus group spread. We provide snapshots representing the dispersal pattern for 1.9 Myr (i), 1.4 Myr (ii), 375,000 ybp (iii) and the present (iv). Lines represent MCC phylogeny branches with heights representing branch length. Branch colors are indicative of each differentiated lineage: *C. ibicuiensis* (blue), *C. minutus* (red), *C. lami* (green), Corrientes group (orange), *C. pearsoni* complex (light blue) and *C. torquatus* (pink). The uncertainty on the location of each ancestral node is represented by green transparent polygons showing the 80% HPD regions. The maps are based on satellite pictures made available in Google Earth (http://www.earth.google.com). A dynamic visualization of the spatio-temporal reconstruction can be explored in Supplementary file S3.

sampling of the torquatus group populations to infer the evolution of its lineages in space and time.

Sequences were aligned with CLUSTAL X2 (Larkin et al., 2007). We partitioned the cyt-b sequence into 1st+2nd and 3rd codon positions separately. Substitution saturation for each partition was assessed with DAMBE (Xia and Xie, 2001) performing a test introduced by Xia and collaborators (Xia et al., 2003; Xia and Lemey, 2009). To use as priors, we estimated substitution models for each partition with MrModeltest 2.3 (Nylander, 2004).

Multi-calibrated timetree

We retrieved nucleotide sequences of the complete (or partial, when not available) cytochrome b (cyt-b) gene from GenBank (Supplementary Table S1) of the Octodontinae subfamily as well as the Abrocomidae, Echimyidae, Myocastoridae and Capromyidae families. Regarding *Ctenomys*, we included 31 sequences representing the torquatus group and 58 additional sequences comprising more than 50 species of the genus (included in Parada et al., 2011 and references therein). We included representative samples from the torquatus group: one representative of each of the seven main clades of the Corrientes group (Caraballo et al., 2012), 8 sequences from different populations of the *C. pearsoni* complex (Tomasco and Lessa, 2007; Caraballo et al., 2016), 7 sequences representing the widespread distribution of *C. torquatus* (Roratto et al., 2015), 4 sequences from each of four localities of *C. ibicuiensis* (Freitas et al., 2012) and 4 sequences from *C. minutus* and the only cyt-b sequence available in the Genebank from *C. lami* (Lopes et al., 2013). The complete multi-calibrated dataset has 132 terminals.

We evaluated the use of 2 sets that differed in the number of fossil calibrations for divergence time estimation. The broadest set included 7 calibrated nodes starting at Octodontoidea and we also tested a subset of 4 calibrated nodes within Octodontidae (Supplementary Figure S1 and Supplementary File S1). Fossil calibrations relied on recent cladistic studies involving both living and fossil taxa (Vucetich et al., 2015; Verzi et al., 2016 and references therein). Supplementary File S1 describes minimum and maximum ages assigned to each calibrated node, with reference to fossil taxa, locality and stratigraphic level, as well as geological age estimates. To account for uncertainty in node calibrations, we applied lognormal priors. Minimum ages were established taking into account the oldest record of the crown group (with

acceptance of the majority of cladistic approaches). We applied soft maximum bounds as the rear 5% of the lognormal distribution using dates from the youngest fossil assemblage that did not include fossils belonging to the calibrated group. All calibrated nodes were forced to be monophyletic in the analysis.

We estimated divergence times in BEAST 2.4.4 (Bouckaert et al., 2014) implementing a relaxed lognormal clock model and the Calibrated Birth-Death tree prior (Heled and Drummond, 2014), which accounts for lineages origination and extinction. We ran BEAST on the CIPRES Science Gateway (Miller et al., 2010) using two different datasets: a) 7 calibrated nodes (nodes A, B, C, D, E, F, G, see Supplementary Figure S1 and Supplementary File S1); b) 4 calibrated nodes (nodes D, E, F, G, see Supplementary Figure S1 and Supplementary File S1). For each dataset we performed two independent runs for $3x10^8$ MCMC generations sampling every 30,000 generations, with a burnin of 25% and also performed an extra run for each set sampling from the prior. We used Tracer 1.6.0 (Rambaut et al., 2014) to determine posterior distribution convergence which indeed was reached in all runs (marginal distributions between runs were totally overlapped for all parameters; the lower ESS values were 487 and 696 for datasets a and b respectively). Log files and trees were combined using LogCombiner 2.4.4, and trees were summarized with the maximum clade credibility (MCC) option using Tree Annotator 2.4.4 (Bouckaert et al., 2014).

Bayesian phylogeographical analysis

We conducted a continuous diffusion analysis of the torquatus group to infer simultaneously the evolutionary history in time and space from molecular sequence data. We implemented the GEO_SPHERE package (Bouckaert, 2016) in BEAST 2.4.4 (Bouckaert et al., 2014), which assumes that taxa migrate through a random walk over a sphere, relaxing the diffusion process by accommodating branch-specific variation in dispersal rates (Lemey et al., 2010). We ran BEAST on the CIPRES Science Gateway (Miller et al., 2010).

We included 95 cyt-b sequences representing all populations of the torquatus group available in GenBank and a sequence of *Ctenomys rionegrensis* as outgroup. Sampling locations and geographic coordinates are shown in Supplementary Table 2. We applied random "jittering" (window size 0.01%) to geographical coordinates to avoid possible conflicts derived from using different sequences from identical sampling sites.

We used a clock rate prior, based on the maximum and minimum values of the 95% highest posterior density (HPD) of rates estimated for internal nodes of the torquatus group in the multi-calibrated analysis: 0.0049 – 0.0349 substitutions per site per million years (s/s/My) (Mean: 0.017 s/s/My). A lognormal clock and a Coalescent Bayesian Skyline tree prior were set in the analysis. Two independent runs for $4x10^8$ MCMC generations sampling every 40,000 generations, with a burnin of 25% were performed. Convergence diagnostics were carried out using Tracer 1.6.0, log files were combined using LogCombiner 2.4.4 and MCC trees were annotated with TreeAnnotator 2.4.4. To achieve convergence we set a maximum bound of 2.0 for the standard deviation of the geographic diffusion prior (R. Bouckaert, personal communication).

To provide a spatial projection, we used SPREAD 1.0.6 (Bielejec et al., 2011) to convert the MCC tree, inferred 80% HPD node locations and mean node heights into a keyhole markup language (KML) file. Supplementary File S3 contains the resulting interactive visualization.

Rates of chromosomal variability

We took into account chromosomal rearrangements that modify diploid and/or fundamental numbers caused by Robertsonian fusions/fissions and/or pericentric inversions. To do so, we defined the macrostructural karyotypic diversification (mKD) within a lineage as the number of different karyomorphs following Martínez et al. (2016). Microstructural rearrangements require chromosome banding and/or painting techniques to be detected, but these studies are not complete for all members of the torquatus group. The rate of karyotypic diversification for a lineage was calculated dividing the mKD values by its estimated age (obtained through the multi-calibrated timetree analysis). The units for the mKD rate within a lineage are numbers of karyomorphs per million years.

Results

Sequence analysis

No deletions, insertions or stop codons were either observed in the 1140 bp alignment of the 132 sequences encompassing all *Ctenomys* and the rest of the Octodontoidea representatives, or in the alignment of 95 sequences of the torquatus group. No saturation

was revealed by the substitution saturation test implemented for the 1st+2nd codon positions or for the 3rd codon position. Supplementary File S2 lists the number of variable and parsimony informative sites, the results of Xia's test for substitution saturation and the substitution model estimated by MrModeltest for each dataset and partition.

Multi-calibrated timetree

We recovered phylogenetic relationships among Octodontoidea families congruent with previously published phylogenies (Upham and Patterson, 2012, 2015), as well as among Octodontidae and Octodontinae representatives (Honeycutt et al., 2003; Opazo, 2005; Upham and Patterson, 2012, 2015; Suárez-Villota et al., 2016) (Supplementary Figure S1). Within *Ctenomys*, we recovered the main 8 groups published by Parada et al. (2011) plus some well supported intergroup relationships (Figure 2): 1) the torquatus group being sister to the (mendocinus, talarum) group; 2) the boliviensis group is sister to the also Bolivian taxa, (*C. steinbachi*, (*C. andersoni*, *C. yatesi*, *C. erikacuellarae*)) (Gardner et al., 2014). With low posterior support (0.66) *C. sociabilis* results sister to *C. tuconax* and together with the frater group are basal to the rest of the genus. These intergroup relationships had also been recovered by Roratto et al. (2015).

Within the torquatus group, phylogenetic relationships were recovered in concordance to previous studies (Freitas et al., 2012; Roratto et al., 2015; Caraballo et al., 2016). Namely, the (Corrientes group, *C. pearsoni* complex), (*C. torquatus*, (*C. minutus*, *C. lami*)), and *C. ibicuiensis* clades split apart from a basal polytomy (Figure 2). It is worth noting that in the coalescent analysis (Supplementary Figure S2), the basal polytomy is resolved in favour of a basal split of *C. ibicuiensis* (with 0.66 posterior value).

The timetree of the main clades among *Ctenomys* and main lineages of the torquatus group under dataset a (7 calibrations) is shown in Figure 2. The two datasets (a: 7 calibrations, b: 4 calibrations) are equivalent in terms of overlapping 95% credibility intervals (Figure 3), although estimations were narrower when using dataset a. In the following part of the study, we consider our estimates obtained with dataset a (7 calibrations) since it yielded more precise dates.

The crown *Ctenomys* most recent common ancestor (MRCA) appeared at 5.88 million years from the present (Myr) (95% HPD: 4.32-7.54 Myr). The origin of the torquatus group is dated at 1.78 Myr (1.25 –
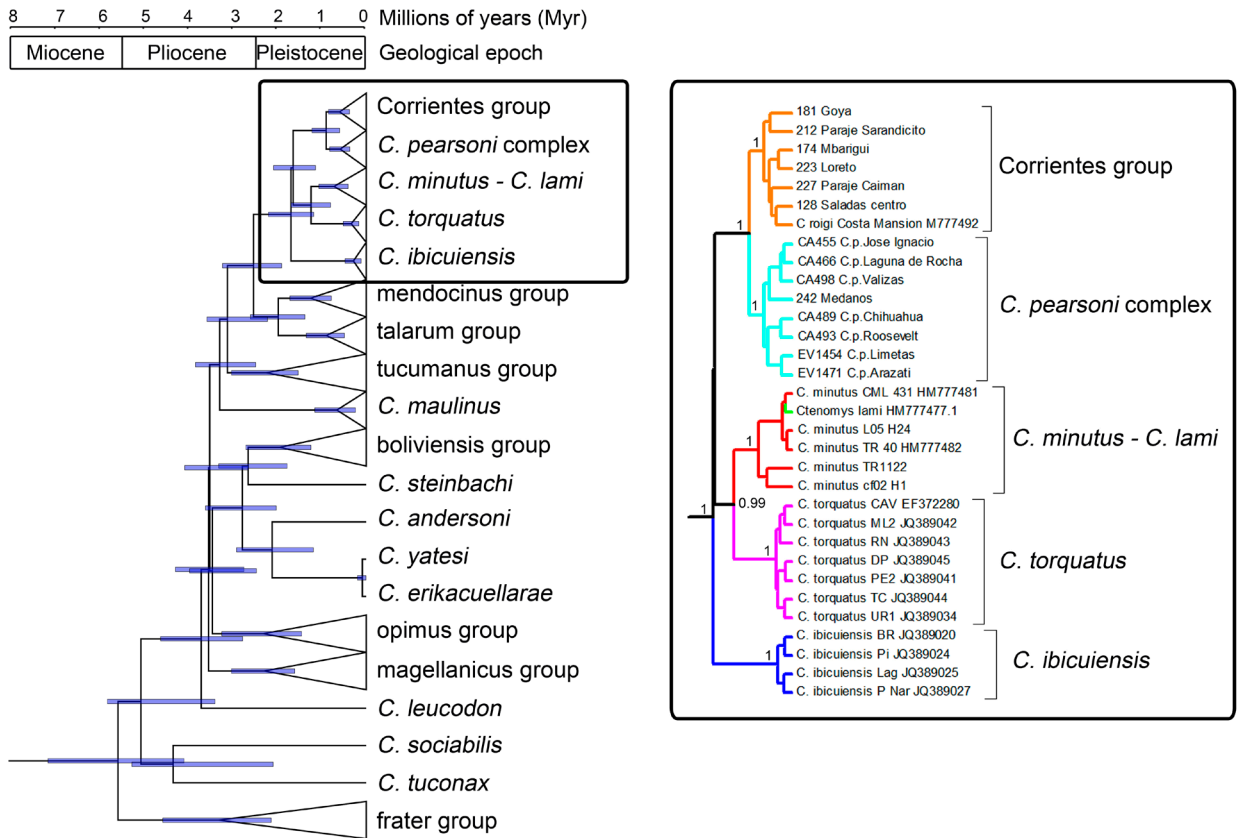
Figure 2. Timetree showing main lineages within *Ctenomys* under dataset a. Node bars correspond to 95% credibility intervals. The timescale showing geological epochs is from Gradstein et al. (2008).

2.32 Myr). Immediately, two basal splits occurred. At 1.20 - 2.32 Myr, three main clades took origin: the (Corrientes group, *C. pearsoni* complex) clade, the (*C. torquatus*, (*C. lami*, *C. minutus*)) clade and the *C. ibicuiensis* clade. The split between the Corrientes group and the *C. pearsoni* complex is dated to 950,000 years before present (630,000 - 1,290,000 ybp), while the split between *C. torquatus* and the (*C. minutus*, *C. lami*) clade occurred earlier at 1.30 Myr (0.84 - 1.79 Myr). Although *C. ibicuiensis* is the most basal diverging species, its MRCA is relatively young, being dated to 300,000 (120,000 - 500,000 ybp). The *C. torquatus* MRCA is dated at 360,000 ybp (180,000 - 540,000 ybp) while (*C. minutus*, *C. lami*) MRCA is dated at 760,000 ybp (430,000 - 1,120,000 ybp). The MRCA of the *C. pearsoni* complex is dated at 615,000 ybp (390,000 - 870,000 ybp) while the Corrientes group MRCA is dated to 630,000 ybp (400,000 – 900,000 ybp) (Figure 2).

Bayesian phylogeographical analysis

Divergence time estimates and phylogenetic relationships of the species and species complexes of the torquatus group were recovered in the coalescent analysis based on 94 sequences representing its geographic and haplotypic diversity (Supplementary Figure S2). Divergence times 95% HPD intervals were larger than those obtained in the multi-calibrated analysis, probably as a result of the use of a broad prior on the clock rate (see Materials and Methods).

A remarkable aspect that emerges from the topological inspection of the tree is that the Entrerrianan populations of Paso Vera and San Joaquín de Miraflores, which had been alleged to belong to *C. dorbignyi* (Corrientes group) (Argüelles et al., 2001; Bidau, 2015) are allied to the also Entrerrianan population of Médanos, and form part of the *C. pearsoni* complex confirming our recent findings (Caraballo and Rossi, 2017).

The ancestral location of the torquatus group MRCA and its subsequent spread throughout its territory are shown in Figure 1B (See an interactive phylodynamic reconstruction in Supplementary File S3). The estimated ancestral area of the torquatus group MRCA spans over the western/central northern region of Uruguay and the southern/central region of Rio Grande do Sul state (Brazil), sharing part of the present distribution of *C.*

torquatus (but also spanning over the area of occupancy of *C. ibicuiensis*) (Figure 1B.i). At 1.8 Myr, the three basal lineages split, initiating different dispersal routes (Figure 1B.ii). The (*C. pearsoni* complex, Corrientes group) ancestral lineage extended to the west, splitting at around 1.0 Myr, while the coastal (*C. lami, C. minutus*) ancestral lineage dispersed to the east. The lineage leading to *C. ibicuiensis* would have remained within
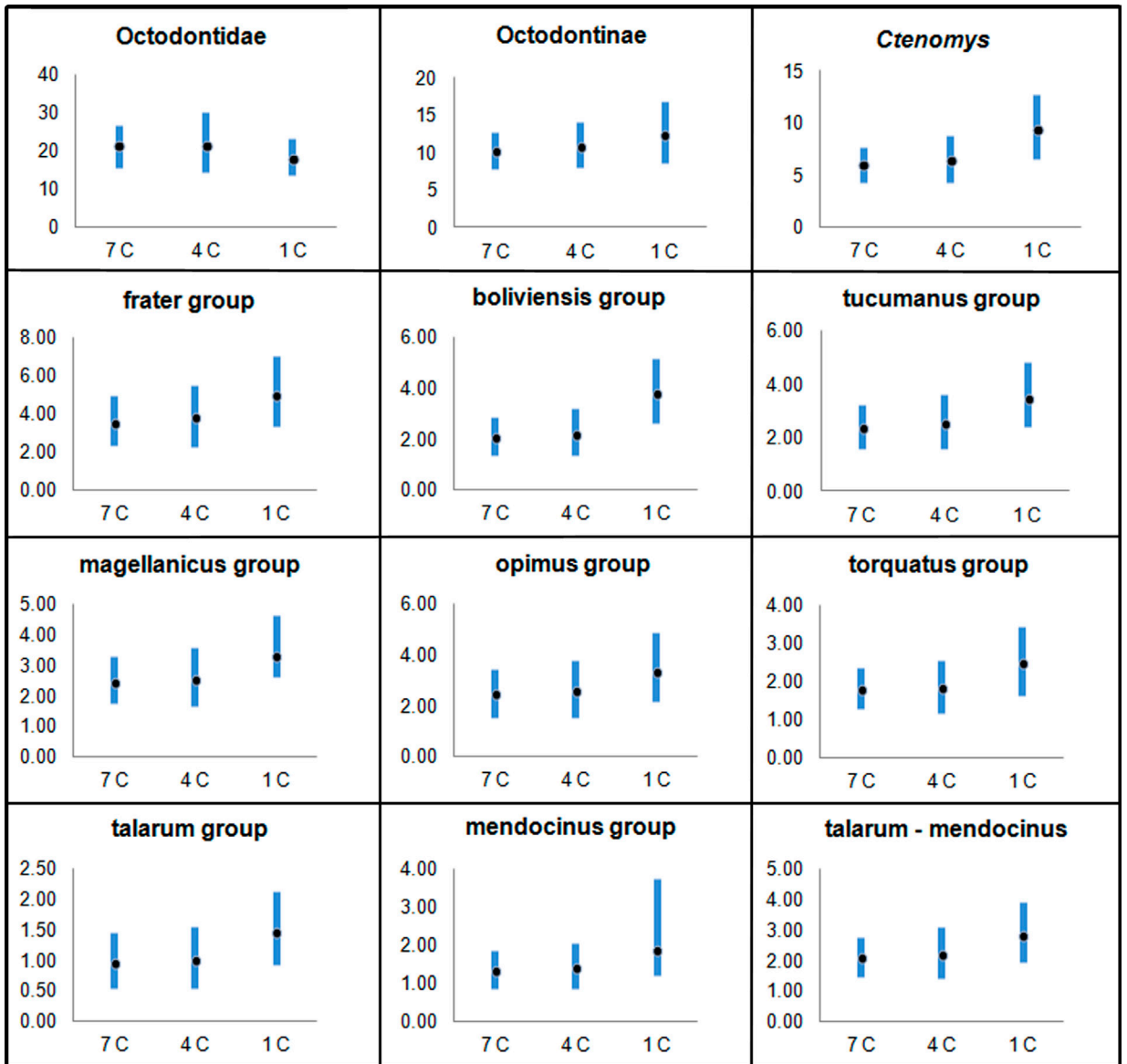

Figure 3. Divergence time estimations obtained with datasets differing in number of taxa and fossil calibrations. Bars represent 95% highest posterior densities, while dots represent mean values. In the horizontal axis, the legends 7 C and 4 C correspond to 7 calibrated nodes (dataset a) and 4 calibrated nodes (dataset b), respectively, while 1 C are the results obtained by Parada et al. (2011), using 1 calibrated node and partial sampling of Octodontinae and Echimyidae (including Myocastoridae and Capromyidae). The vertical axis is expressed in Million years.

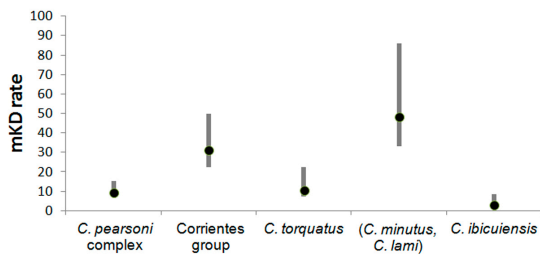| Species/Group	Mean age (Myr)	95% HPD range (Myr)		mKD
		Min	Max	
C. pearsoni complex	0.62	0.39	0.87	6
Corrientes group	0.63	0.40	0.90	20
C. torquatus	0.36	0.18	0.54	4
(*C. minutus*, *C. lami*)	0.76	0.43	1.12	37
C. ibicuiensis	0.30	0.12	0.50	1

Figure 4. Macrostructural karyotypic diversification (mKD) rates in the five main lineages of the *torquatus* group. Rates were calculated as the number of different karyomorphs within each lineage divided by its age (mean and 95% HPD) (mKD rate units are number of karyomorphs per Million years).

the ancestral area of the group. Between 1.00 - 0.45 Myr, the *C. pearsoni* complex, the Corrientes group and the (*C. minutus*, *C. lami*) clade underwent an augmented cladogenesis accompanied by a range expansion along most of their present territories (Figure 1B.iii). In this period at least two times the Uruguay River must have been crossed by the ancestral tuco-tuco stocks of the Corrientes group and the Entrerrianan representatives of the *C. pearsoni* complex. Around 300,000 ybp, *C. torquatus* went through a dramatic range expansion along with a profuse cladogenesis that lasted up to around 40,000 ybp (Figure 1B.iv). The overall range expansion of the torquatus group is also reflected by a Lineages Through Time plot which shows a shift in diversification rate around 780,000 ybp (Supplementary Figure S3).

Rates of chromosomal diversification

As mentioned, differences in karyological diversity are a conspicuous feature of the torquatus group. For instance, *C. lami* depicts the highest chromosomal variability in the genus (Freitas, 2007); the Corrientes group also shows wide chromosomal differences among its lineages (Caraballo et al., 2015 and references therein). On the other extreme, a unique karyotype was found among the populations of the geographically restricted *C. ibicuiensis* (Freitas et al., 2012). Chromosomal divergence within each lineage

could be biased by the number of sampled individuals and/or populations. However, this is not the case, since, for instance, *C. torquatus* has the highest number of studied populations (34) (Roratto et al., 2015) although its mKD value is relatively low (4). In the other extreme, 16 neighbouring *C. lami* demes harbor 26 different karyomorphs (Freitas, 2007) (Figure 4).

The estimation of the ages of the MRCA of each lineage enabled us to assess their rates of chromosomal evolution. Figure 4 shows the mKD values, the MRCA ages and the rates of mKD (along with their uncertainty given by the 95% HPD ranges of the MRCA ages) for the five main lineages of the torquatus group. The clade (*Ctenomys minutus*, *C. lami*) and the Corrientes group depict the higher rates of mKD, being 48.7 and 31.7 karyomorphs/Myr, respectively. The *C. pearsoni* complex and *C. torquatus* show intermediate values, being 9.8 and 11.1 karyomorphs/Myr. The young *C. ibicuiensis* with only one karyotype displays, as expected, the minimum rate of mKD (3.3 karyomorphs/Myr).

Discussion

Multi-calibrated timetree

In agreement with both, simulation (Duchêne et al., 2014; Soares and Schrago, 2015) and empirical studies (Bibi, 2013; Zheng and Wiens, 2015), our study confirms that precision in divergence time estimation depends on the number of calibrations. The inclusion of a higher number of calibrated nodes (7 vs 4) in the analysis yielded narrower time estimates confidence intervals (Figure 3). It is worth noting that extra calibrated nodes in dataset a in comparison with dataset b are placed at deeper nodes and that the inclusion of such calibrations is associated with higher divergence time precision values in simulation studies (Mello and Schrago, 2013).

Mean divergence times inferred in this study are congruent with those published in previous studies (Table 1). The most comparable analysis in terms of included taxa and loci was the study of Parada et al. (2011), also based on cyt-b sequences including representatives of all *Ctenomys* species groups. The main differences between this study and Parada et al. (2011) were the number of calibrated nodes (7 vs 1) and outgroup sampling (9 sequences in Parada et al. 2011 vs 42 sequences in the present study, Supplementary Table S1). Even though our estimates are roughly

equivalent in terms of overlapping credibility intervals to those obtained by Parada et al. (2011), the ranges obtained using 7 calibrations are considerably narrower (Figure 3). As discussed above, these results are congruent since precision in node age estimates is increased mainly by adding more calibrations.

Not only are the estimates obtained with 7 calibrations more precise compared to those obtained with 4 calibrations (this study) and 1 calibration (Parada et al., 2011) but also mean values are different. This difference poses a question about accuracy. We will consider some hints derived from data and results comparison together with results from theoretical approaches. Notably, mean ages take slightly higher values when using 4 compared with 7 calibrated nodes. As mentioned above, higher levels of accuracy are obtained when using multiple calibrated (Bibi, 2013; Duchêne et al., 2014; Soares and Schrago, 2015) and adjacent nodes (Linder et al., 2005), and when these

	This study	Suárez-Villota et al. 2016	Upham & Patterson 2015	Roratto et al. 2015	Upham & Patterson 2012	Parada et al. 2011	Opazo 2005
Crown Octodontoidea	29.30 (27.3-32.48)	-	25.6 (23.1-27.9)	-	26.8 (24.8-28.9)	-	20.6 (18.2-23.0)
Crown Abrocomidae	10.40 (6.15-14.67)	-	8.4 (7.2-15.0)	-	0.3 (0-1.8)	-	-
Octodontidae-Echimyidae	26.33 (23.13-29.54)	-	23.6 (21.4-25.8)	-	25.3 (24.6-26.7)	23.18 (18.2-28.6)	17.5 (15.3-19.7)
Crown Echimyidae	21.36 (20.6-22.50)	-	18.2 (17.1-19.3)	-	18.8 (17.7-20.6)	-	-
Octodontidae	21.35 (15.59-26.69)	-	18.9 (15.7-22.1)	11.17 (10.20-12.13)	19.1 (14.3-23.5)	17.97 (13.5-23.0)	15 (12.9-17.1)
Octodontinae	10.15 (7.83-12.67)	11.08 (7.25-16.41)	8.8 (7.3-10.4)	-	9.0 (6.7-11.6)	12.34 (8.4-16.7)	7.79 (6.29-9.29)
Octo-Pipa-Tympa	2.63 (2.26-3.06)	6.10 (3.40-9.45)	5.4 *	-	-	-	4.28 (2.48-6.08)
Aconaemys-Spalacopus	5.46 (5.07-6.00)	3.23 (2.0-4.8)	3.1 *	-	-	-	2.22 (1.57-2.87)
Ctenomys	5.88 (4.32-7.54)	-	6.0 (4.6-7.6)	5.64 (4.38-6.98)	4.3 (2.2-7.4)	9.22 (6.44-12.6)	-
torquatus group	1.78 (1.25-2.32)	-	-	-	-	2.46 (1.6-3.4)	-
C. torquatus	0.36 (0.18-0.54)	-	-	0.24 (0.15-0.37)	-	-	-

Clock model	Uncorrelated Lognormal	Uncorrelated Lognormal	Uncorrelated Lognormal	Uncorrelated Lognormal	Uncorrelated Lognormal	Uncorrelated Lognormal	Lognormal
Branching rates prior	Birth-Death process	Not informed	Birth-Death process	Yule process	Yule process	Yule process	N.A.
Calibrations	7	1	22	3	5	1	1
Calibration prior	Lognormal	Lognormal	Lognormal	Normal/Lognormal distributions	Lognormal	Range (uniform)	Range (uniform)
Octodontoidea sampling	Complete	Incomplete	Complete	Incomplete	Complete	Incomplete	Incomplete
Number of loci	1 (cyt-b)	2 (GHR, 12s rRNA)	5 (cyt-b, GHR, vWF, 12s rRNA, RAG1)	1 (cyt-b)	4 (GHR, vWF, 12s rRNA, RAG1)	1 (cyt-b)	2 (12s rRNA, GHR)

Table 1. Divergence time estimations within Octodontidae compared among studies. All estimations are expressed as mean divergence times (and confidence intervals) in million years (Myr). Results from this study correspond to the timetree shown in Figure 2. The lower part of the table shows relevant information for analyses comparisons, such as clock model, branching and calibration priors, taxon sampling and number of loci included in each study. Asterisks (*) indicate that only mean ages are informed. The acronym *Octo-Tympa-Pipa* stands for the MRCA of *Octomys*, *Tympanoctomys* and *Pipanacoctomys*.

calibrations occupy a deep position in the phylogeny (Mello and Schrago, 2013), suggesting that results using dataset a may be the most accurate estimates overall. Furthermore, we remark that increased taxon sampling also improves molecular dating accuracy (Heath et al., 2008; Schulte, 2013; Soares and Schrago, 2015).

Origin and dispersion of the torquatus group

The inferred location of the ancestral stock of the torquatus group is placed in north-western Uruguay / south-western Río Grande do Sul state (Brazil) at around 2 Myr (Figure 1B.i). From this stock, lineages leading to *C. pearsoni* complex, the Corrientes group and (*C. minutus*, *C. lami*) dispersed to non-overlapping distributions, initiating an independent evolutionary path (Figure 1B. ii and iii). In turn, *C. ibicuiensis* and the ancestor of *C. torquatus* remained close to the ancestral location of the group for a long period of time (Figure 1B. ii, iii and iv).

With exception of *C. ibicuiensis* all species and species complexes of the torquatus group have experienced substantial range expansions in the last 800,000 – 700,000 years. As mentioned above, the most dramatic case is the one of *C. torquatus*, which has gone through an explosive cladogenesis accompanied with a considerable range expansion for the last 200,000 years, becoming the most widespread species of the group. These results are in agreement with a fine-scale analysis of the *C. torquatus* populations which indicate a pattern of recent demographic expansion (Roratto et al., 2015). In addition, haplotypic uniqueness of peripheral populations of the species distribution, in contrast to a more widespread and frequent haplotype in the central/north-eastern distribution of *C. torquatus*, suggests that the latter would reflect the ancestral distribution of the species (Roratto et al., 2015). These findings are in congruence with the ancestral location reconstruction presented in this study (Figure 1B, Supplementary File S3).

The Uruguay River as a barrier

The Uruguay is the third among the largest rivers of South America. It has its headwaters at tropical Brazilian plateau and flows along 1,838 km from north to south, with a drainage area of about 365,000 km² (Di Persia et al., 1986). The Uruguay River separates the Argentinean Mesopotamian region from Brazil and Uruguay and probably originated in the

Quaternary as a consequence of tectonic movements associated with the elevation of mountains in South Brazil. It is a large river, with an average discharge of 4,500 m³/s, with a minimum width of 30 m at Saltos del Moconá, and a maximum of 12 km at its mouth in the confluence with the Río de la Plata (Di Persia et al., 1986). Its dimensions and flow magnitude make the Uruguay River a putative barrier to gene flow in non-volant mammals. However, the paraphyletic nature of the Argentinean populations from Entre Ríos and Corrientes provinces indicates that tuco-tucos should have been able to cross the Uruguay River at least twice during the colonization of the Argentinean Mesopotamia.

The ability to sporadically disperse across large rivers would be widespread among mammals. In a large-scale analysis based on divergence patterns using cyt-b sequences of several non-volant mammals from the Amazon basin, Patton et al. (2000) found no evidence to support that the Juruá River, one of the main affluent rivers of the Amazon River, would act as an important barrier, suggesting that large rivers could be more likely to be crossed than expected. In a study based on RAPD (Random Amplified Polymorphic DNA) data, the cricetid rodent *Oligoryzomys* showed no structure at both banks of the Uruguay River at the proximities of the headwater (Mossi et al., 2014), indicating that it would not be acting as a strong barrier to gene flow. Regarding tuco-tucos, the diversification along but not across rivers demonstrated that *C. torquatus* may have been able to cross the also large Ibicuí, Vacacaí and Jacuí rivers during a period of dry climate (Roratto et al., 2015). Furthermore, the species *C. rionegrensis* is also distributed at both east and west of the Uruguay River (Ortells et al., 1990; D'Elía et al., 1999) and must have also been able to cross it, which at the present seems to be an unlikely event. However, the strength of these rivers as barriers would not have been constant along time. Indeed, the region that comprises the torquatus group distribution has gone through profound climate changes associated with glacial events occurred during the early and middle Pleistocene (Rabassa et al., 2005; Bossi et al. 2009). The Ensenadan Stage/Age (1.8 – 0.5 Myr, Dunn et al., 2013) had warm and humid climates, between 1.6 and 1.0 Myr, but in phase with the Great Patagonian Glaciation (1.17 – 1.001 Myr), a colder and drier climate developed between 0.98 and 0.5 Myr, as indicated by a steady decrease in plant and faunal content in the stratigraphic record (Bossi et al., 2009). During this period strong oscillations in temperature

have occurred reaching a relative minimum at 0.78 Myr and an absolute minimum at 0.6 Myr (Bossi et al., 2009). Notably, the crossings through the Uruguay River must have occurred between circa 1 Myr, when the ancestral stock of the *C. pearsoni* complex, Corrientes group split into two lineages that dispersed differentially, and circa 500,000 Myr, the time when there were established populations in Entre Ríos and Corrientes provinces (Supplementary File S3). Hence, tuco-tucos must have been able to cross the Uruguay River during a cold and dry period when it was weaker in strength as a dispersal barrier.

Chromosomal diversification

Ctenomys is considered a paradigmatic example of chromosomal evolution among mammals (Reig and Kiblisky, 1969; Reig et al., 1990). Semi-isolated demes, small population sizes, and limited vagility are life history traits that may have facilitated the fixation of chromosomal rearrangements in these rodents (Reig et al., 1990). However, different patterns of chromosomal dynamics could be observed in the species groups of this genus (Cook et al., 1990; Ortells et al., 1990; Massarini et al., 1991; Freitas, 2007). Since ecological and life history features are shared among tuco-tucos, differences in patterns of chromosomal evolution should be explained by intrinsic genome dynamics rather than by ecological traits. Nevertheless, in widespread species with highly structured populations, a higher rate of chromosomal rearrangement fixation would be expected in populations located at extremes of the distribution (Lande, 1985).

As mentioned above, mKD values and its rates differ in one order of magnitude among the 5 lineages of the torquatus group (Figure 4). Chromosomal evolution in *Ctenomys* has been related to differential dynamics (stasis, amplification and/or deletion) of RPCS (repetitive PvuII Ctenomys sequence), its major satellite DNA (Slamovits et al., 2001; Ellingsen et al., 2007) within the genus. It is worth noting that when we quantified RPCS copy number among individuals and populations of the Corrientes group we found differences up to one order of magnitude even within populations (Caraballo et al., 2010). Beyond the mechanism by which RPCS could cause chromosomal rearrangements in each case, extensive deletions, amplifications and re-localizations within the genome would undoubtedly alter chromosome structure.

As mentioned above, it is expected that the amplitude of the geographic range influences the probability of fixation of chromosomal changes. This seems to be the case for the Corrientes group, which has an ample distribution area (Figure 1A). In this group, high chromosomal variability (Caraballo et al., 2015) and profuse RPCS expansions and contractions (Caraballo et al., 2010) co-occurred in a relatively short period of time (0.63 Myr). However, *C. lami* would be an exception: 26 karyotypes are distributed in a restricted area in the coastal region of the southern part of Brazil (Figure 1A). *Ctenomys torquatus* also deserves attention because it depicts a relatively low rate of mkD (Figure 4) albeit being the most widespread species of the group (Figure 1A). Since the recent explosive expansion of the plesiomorphic cytotype (0.20 - 0.35 Myr), only a few new karyotypes resulted fixed in the periphery of its geographical distribution (Roratto et al., 2015, Supplementary File S3). In conclusion, the karyotypic diversity of the torquatus group is the outcome of the interplay of several factors acting at different biological levels: the proneness of the genome to chromosomal rearrangements, the elapsed time since the MRCA, and also the extent of dispersion of each lineage over the territory.

Concluding remarks

The present study manifests the importance of integrating spatial, temporal, phylogenetic, and paleoclimatologic dimensions to perform inferences about evolutionary processes. Significant questions about the patterns of dispersal and territorial colonization, cladogenesis and chromosomal diversification could only be interpreted under such a multidimensional scenario.

References

Anonymous. The IUCN Red List of Threatened Species. Version 2016-3. <www.iucnredlist.org>. Downloaded on 28 April 2017.

Argüelles CF, Suárez P, Giménez MD, Bidau CJ. 2001. Intraspecific chromosome variation between different populations of *Ctenomys dorbignyi* (Rodentia, Ctenomyidae) from Argentina. *Acta Theriologica* 46: 363–373.

Bibi F. 2013. A multi-calibrated mitochondrial phylogeny of extant Bovidae (Artiodactyla, Ruminantia) and the importance of the fossil record to systematics. *BMC Evolutionary Biology* 13: 166.

Bidau C. 2015. Family Ctenomyidae Lesson, 1842. Pp. 818–877 in: JL Patton, UFJ Pardiñas, G D'Elía, eds, *Mammals of South America, Volume 2: rodents*. University of Chicago Press, Chicago, USA.

Bielejec F, Rambaut A, Suchard MA, Lemey P. 2011. SPREAD: spatial phylogenetic reconstruction of evolutionary dynamics. *Bioinformatics* 27: 2910-2912.

Bloomquist EW, Lemey P, Suchard MA. 2010. Three roads diverged? Routes to phylogeographic inference. *Trends in Ecology and Evolution* 25: 626-632.

Bossi J, Ortiz A, Perea D. 2009. Pliocene to middle Pleistocene in Uruguay: a model of climate evolution. *Quaternary International* 210: 37-43.

Bouckaert R, Heled J, Kühnert D, ... Drummond A. 2014. BEAST 2: a software platform for Bayesian evolutionary analysis. *PLOS Computational Biology* 10: e1003537.

Bouckaert R. 2016. Phylogeography by diffusion on a sphere: whole world phylogeography. *PeerJ* 4: e2406. http://doi.org/10.7717/peerj.2406

Caraballo DA, Abruzzese GA, Rossi MS. 2012. Diversity of tuco-tucos (*Ctenomys*, Rodentia) in the Northeastern wetlands from Argentina: Mitochondrial phylogeny and chromosomal evolution. *Genetica* 140: 125–136.

Caraballo DA, Belluscio PM, Rossi MS. 2010. The library model for satellite DNA evolution: a case study with the rodents of the genus *Ctenomys* (Octodontidae) from the Iberá marsh, Argentina. *Genetica* 138: 201-1210.

Caraballo DA, Jablonski PC, Rebagliati PJ, Rossi MS. 2015. Chromosomal variability in tuco-tucos (*Ctenomys*, Rodentia) from the argentinean northeastern wetlands. *Mastozoología Neotropical* 22: 289–301.

Caraballo DA, Rossi MS. 2018. Integrative lineage delimitation in rodents of the *Ctenomys* Corrientes group. *Mammalia*, 82(1), pp. 35-47. Retrieved 23 Feb. 2018, from doi:10.1515/mammalia-2016-0162

Caraballo DA, Tomasco IH, Campo DH, Rossi MS. 2016. Phylogenetic relationships between tuco-tucos (*Ctenomys*, Rodentia) of the Corrientes group and the *C. pearsoni* complex. *Mastozoología Neotropical* 23: 39-49.

Cook JA, Anderson S, Yates TL. 1990. Notes on Bolivian mammals. 6, The genus *Ctenomys* (Rodentia, Ctenomyidae) in the highlands. *American Museum Novititates* 2980:1–27

D'Elía G, Lessa EP, Cook JA. 1999. Molecular phylogeny of tuco- tucos, genus *Ctenomys* (Rodentia: Octodontidae): evaluation of the mendocinus species group and the evolution of asymmetric sperm. *Journal of Mammalian Evolution* 6:19–38.

Di Persia DH, Neiff JJ, Olazarri J. 1986. The Uruguay River system. Pp. 599-622 in: BR Davies, KF Walker, eds, *The Ecology of River Systems*. *Monographiae Biologicae*, vol 60. Springer, Dordrecht.

Drummond AJ, Ho SYW, Phillips MJ, Rambaut A. 2006. Relaxed phylogenetics and dating with confidence. *PLOS Biology* 4: e88.

Drummond AJ, Rambaut A. 2007. BEAST: Bayesian evolutionary analysis by sampling trees. *BMC Evolutionary Biology* 7: 214.

Duchêne S, Lanfear R, Ho SYW. 2014. The impact of calibration and clock-model choice on molecular estimates of divergence times. *Molecular Phylogenetics and Evolution* 78: 277–289.

Dunn RE, Madden RH, Kohn MJ, Schmitz MD, Strömberg CA, Carlini AA, ... Crowley J. 2013. A new chronology for middle Eocene–early Miocene South American land mammal ages. *Geological Society of America Bulletin* 125: 539-555.

Edwards CJ, Suchard MA, Lemey P, Welch JJ, Barnes I, Fulton TL, ... Valdiosera CE. 2011. Ancient hybridization and an Irish origin for the modern polar bear matriline. *Current Biology* 21: 1251-1258.

Ellingsen A, Slamovits CH, Rossi MS. 2007. Sequence evolution of the major satellite DNA of the genus *Ctenomys* (Octodontidae, Rodentia). *Gene* 392:283–290.

Fernandes FA, Gonçalves GL, Ximenes SSF, Freitas TRO. 2009. Karyotypic and molecular polymorphisms in the *Ctenomys torquatus* (Rodentia: Ctenomyidae): taxonomic considerations. *Genetica* 136: 449–459.

Freitas TRO, Fernandes FA, Fornel R, Roratto PA. 2012. An endemic new species of tuco-tuco, genus *Ctenomys* (Rodentia: Ctenomyidae), with a restricted geographic distribution in southern Brazil. *Journal of Mammalogy* 93: 1355–1367.

Freitas TRO. 1995. Geographic distribution and conservation of four species of the genus *Ctenomys* in southern Brazil. *Studies on Neotropical Fauna and Environment* 30: 53–59.

Freitas TRO. 2007. *Ctenomys lami*: The highest chromosome variability in *Ctenomys* (Rodentia, Ctenomyidae) due to a centric fusion-fission and pericentric inversion system. *Acta Theriologica* 52: 171-180.

Gardner SL, Salazar-Bravo J, Cook JA. 2014. New species of *Ctenomys* Blainville, 1826 (Rodentia: Ctenomyidae) from the Central Valleys of Bolivia. *Special Publications of the Museum of Texas Tech University* 62.

Gradstein FM, Ogg JG, Van Kranendonk M. 2008. On the Geologic Time Scale 2008. *Newsletters on Stratigraphy* 43: 5–13.

Heath TA, Hedtke SM, Hillis DM. 2008. Taxon sampling and the accuracy of phylogenetic analyses. *Journal of Systematics and Evolution* 46: 239–257.

Heled J, Drummond AJ. 2014. Calibrated birth–death phylogenetic time-tree priors for Bayesian inference. *Systematic Biology* 64: 369-383.

Ho SYW, Phillips MJ. 2009. Accounting for calibration uncertainty in phylogenetic estimation of evolutionary divergence times. *Systematic Biology* 58: 367–80.

Honeycutt RL, Rowe DL, Gallardo MH. 2003. Molecular systematics of the South American caviomorph rodents: relationships among species and genera in the family Octodontidae. *Molecular Phylogenetics and Evolution* 26: 476–489.

Hug LA, Roger AJ. 2007. The impact of fossils and taxon

sampling on ancient molecular dating analyses. *Molecular Biology and Evolution* 24: 1889–1897.

Lande R. 1985. The fixation of chromosomal rearrangements in a subdivided population with local extinction and colonization. *Heredity* 54: 323–332.

Larkin MA, Blackshields G, Brown NP, ... Higgins DG. 2007. Clustal W and Clustal X version 2.0. *Bioinformatics* 23: 2947–2948.

Leaché AD, Grummer JA, Miller M, Krishnan S, Fujita MK, Böhme W, ... Ofori-Boateng C. 2017. Bayesian inference of species diffusion in the West African *Agama agama* species group (Reptilia, Agamidae). *Systematics and Biodiversity* 15: 192-203.

Lemey P, Rambaut A, Drummond AJ, Suchard MA. 2009. Bayesian phylogeography finds its roots. *PLOS Computational Biology* 5(9), e1000520.

Lemey P, Rambaut A, Welch JJ, Suchard MA. 2010. Phylogeography takes a relaxed random walk in continuous space and time. *Molecular Biology and Evolution* 27: 1877-1885.

Linder HP, Hardy CR, Rutschmann F. 2005. Taxon sampling effects in molecular clock dating: an example from the African Restionaceae. *Molecular Phylogenetics and Evolution* 35: 569–582.

Lopes CM, Ximenes SSF, Gava A, Freitas TRO. 2013. The role of chromosomal rearrangements and geographical barriers in the divergence of lineages in a South American subterranean rodent (Rodentia: Ctenomyidae: *Ctenomys minutus*). *Heredity* 111: 293–305.

Lukoschek V, Keogh JS, Avise JC. 2012. Evaluating fossil calibrations for dating phylogenies in light of rates of molecular evolution: a comparison of three approaches. *Systematic Biology* 61: 22–43.

Martínez PA, Jacobina UP, Fernandes RV, Brito C, Penone C, Amado TF, Fonseca CR, Bidau CJ. 2016. A comparative study on karyotypic diversification rate in mammals. *Heredity* 118: 366-373.

Massarini A, Barros MA, Ortells MO, Reig OA. 1991. Chromosomal polymorphism and small karyotypic differentiation in Central Argentinian populations of tuco-tucos. *Genetica* 83: 131–144.

Mello B, Schrago CG. 2013. Assignment of calibration information to deeper phylogenetic nodes is more effective in obtaining precise and accurate divergence time estimates. *Evolutionary Bioinformatics* 10: 79–85.

Miller MA, Pfeiffer W, Schwartz T. 2010. Creating the CIPRES Science Gateway for inference of large phylogenetic trees. Pp. 1-8 in: Gateway Computing Environments Workshop (GCE), 2010. IEEE.

Mossi AJ, Coppini VJ, Slaviero LB, Kubiak GB, Lerin LA, Oliveira JV, ... Cansian RL. 2014. Comparison between *Oligoryzomys nigripes* and *O. flavescens* by RAPD and genetic diversity in *O. nigripes* (Rodentia, Cricetidae). *Brazilian Journal of Biology* 74: 704-711.

Nylander J. 2004. MrModeltest v2. Program distributed by the author. Evolutionary Biology Centre, Uppsala University.

Opazo JC. 2005. A molecular timescale for caviomorph rodents (Mammalia, Hystricognathi). *Molecular Phylogenetics and Evolution* 37: 932–937.

Ortells MO, Contreras JR, Reig OA. 1990. New *Ctenomys* karyotypes (Rodentia, Octodontidae) from north-eastern

Argentina and from Paraguay confirm the extreme chromosomal multiformity of the genus. *Genetica* 82:189–201

Parada A, D'Elía G, Bidau CJ, Lessa EP. 2011. Species groups and the evolutionary diversification of tuco-tucos, genus *Ctenomys* (Rodentia: Ctenomyidae). *Journal of Mammalogy* 92: 671–682.

Patton JL, Silva MN, Malcolm JR. 2000. Mammals of the Rio Juruá and the evolutionary and ecological diversification of Amazonia. *Bulletin of the American Museum of National History* 244: 1–306.

Rabassa J, Coronato A, Salemme M. 2005. Chronology of the Late Cenozoic Patagonian glaciations and their correlation with biostratigraphic units of the Pampean region (Argentina). *Journal of South American Earth Sciences* 20: 81–103.

Rambaut A, Suchard MA, Xie D, Drummond AJ. 2014. Tracer v1.6, Available from http://beast.bio.ed.ac.uk/Tracer

Reig OA, Busch C, Ortells MO, Contreras JR. 1990. An overview of evolution, systematics, population biology, cytogenetics, molecular biology and speciation in *Ctenomys*. Pp. 71-96 in: E Nevo and OA Reig, eds, *Evolutionary biology of subterranean mammals*, Alan R. Liss, New York.

Reig OA, Kiblisky P. 1969. Chromosome multiformity in the genus *Ctenomys* (Rodentia, Octodontidae). A progress report. *Chromosoma* 28: 211–244.

Roratto PA, Fernandes FA, Freitas TRO. 2015. Phylogeography of the subterranean rodent *Ctenomys torquatus*: an evaluation of the riverine barrier hypothesis. *Journal of Biogeography* 42: 694-705.

Schulte JA. 2013. Undersampling taxa will underestimate molecular divergence dates: an example from the South American lizard clade Liolaemini. *International Journal of Evolutionary Biology*. Article ID 628467. doi:10.1155/2013/628467

Slamovits CH, Cook JA, Lessa EP, Rossi MS. 2001. Recurrent amplifications and deletions of satellite DNA accompanied chromosomal diversification in South American tuco-tucos (genus *Ctenomys*, Rodentia: Octodontidae): a phylogenetic approach. *Molecular Biology and Evolution* 18:1708–1719.

Soares AER, Schrago CG. 2015. The influence of taxon sampling on Bayesian divergence time inference under scenarios of rate heterogeneity among lineages. *Journal of Theoretical Biology* 364: 31–39.

Suárez-Villota EY, González-Wevar CA, Gallardo MH, Vásquez RA, Poulin E. 2016. Filling phylogenetic gaps and the biogeographic relationships of the Octodontidae (Mammalia: Hystricognathi). *Molecular Phylogenetics and Evolution* 105: 96-101.

Tomasco IH, Lessa EP. 2007. Phylogeography of the tuco-tuco *Ctenomys pearsoni*: mtDNA variation and its implication for chromosomal differentiation. Pp. 859– 882 in: Kelt DA, Lessa EP, Salazar-Bravo J, Patton JL, eds, *The quintessential naturalist: honoring the life and legacy of Oliver P. Pearson*. University of California Press, Berkeley, CA.

Upham NS, Patterson BD. 2012. Diversification and biogeography of the Neotropical caviomorph lineage Octodontoidea (Rodentia: Hystricognathi). *Molecular Phylogenetics and Evolution* 63: 417–29.

Upham NS, Patterson BD. 2015. Evolution of the caviomorph rodents: a complete phylogeny and timetree of living genera.

Pp 63–120 in: AI Vassallo, D Antenucci, eds, *Biology of caviomorph rodents: diversity and evolution*, 1st ed. SAREM Series A, Buenos Aires.

Verzi DH, Olivares AI, Morgan CC, Álvarez A. 2016. Contrasting phylogenetic and diversity patterns in Octodontoid rodents and a new definition of the family Abrocomidae. *Journal of Mammalian Evolution* 23: 93-115.

Vucetich MG, Arnal M, Deschamps CM, Pérez ME, Vieytes EC. 2015. A brief history of caviomorph rodents as told by the fossil record. Pp 11–62 in: AI Vassallo, D Antenucci, eds, *Biology of caviomorph rodents: diversity and evolution*, 1st ed. SAREM Series A, Buenos Aires.

Xia X, Lemey P. 2009. Assessing substitution saturation with DAMBE. Pp 615-630 in: P Lemey, M Salemi, AM Vandamme, eds, *The phylogenetic handbook*, 1st ed. Cambridge University Press, Cambridge.

Xia X, Xie Z, Salemi M, Cheng L, Wang Y. 2003. An index of substitution saturation and its application. *Molecular Phylogenetics and Evolution* 26: 1–7.

Xia X, Xie Z. 2001. DAMBE: software package for data analysis in molecular biology and evolution. *Journal of Heredity* 92: 371–373.

Zheng Y, Wiens JJ. 2015. Do missing data influence the accuracy of divergence-time estimation with BEAST? *Molecular Phylogenetics and Evolution* 85: 41–49.

Online supplementary material

Supplementary Table S1. Classification, DNA sequence accession numbers, and cyt-b coding sequence length of all samples used in the multi-calibrated analysis.

Supplementary Table S2. Names, geographic coordinates, locality and region, DNA sequence accession numbers and bibliographic references of 95 torquatus group and one outgroup samples included in the Bayesian phylogeographic analysis.

Supplementary Figure S1. Phylogeny based on the complete cyt-b sequence of 132 Octodontoid taxa. The node corresponding to *Ctenomys* MRCA is collapsed (expanded in Figure 2). Nodes are annotated with Bayesian posterior probability value. Letters A-G correspond to fossil calibrated nodes as detailed in Supplementary File S1.

Supplementary Figure S2. Phylogeny based on the complete cyt-b sequence of 95 torquatus group sequences representing its geographical and haplotypic diversity. Main lineages nodes are annotated with Bayesian posterior probability value. Branch colors are indicative of each differentiated lineage: *C*. *ibicuiensis* (blue), *C*. *minutus* (red), *C*. *lami* (green), Corrientes group (orange), *C*. *pearsoni* complex (light blue) and *C*. *torquatus* (pink). The timescale units are million years from the present.

Supplementary Figure S3. Log-lineage-through-time plot (LTT plot, full line) describing the dynamics of cladogenesis within the torquatus group over time. The blue shaded area represents the 95% HPD. The black dashed line indicates a shift in diversification rate around 780,000 years before the present.

Supplementary File S1. Detailed justification of minimum and maximum ages assigned to each calibrated node, with reference to fossil taxa, locality and stratigraphic level, as well as geologic age estimates. Each entry begins with the referred clade and its code (matching labeled nodes shown in Supplementary Figure S1), and followed by the lognormal prior's upper 95% range in Millons years (Myr) and the distribution's shape parameters (mean, SD) as implemented in BEAST. Each prior was offset to the minimum age of the oldest crown fossil assigned to that clade that has consensus in recent cladistic studies involving both living and fossil Octodontoid taxa (Vucetich et al. 2015, Verzi et al. 2016 and references therein), and a soft maximum age set at the lower 5% of the prior, using dates from the youngest fossil assemblage that did not include fossils belonging to the calibrated group. SALMAs stand for South American Land Mammal Age.

Supplementary File S2. Number of variable and parsimony informative sites, results of Xia's test for substitution saturation, and substitution model estimated by MrModeltest for each cyt-b dataset and partition.

Supplementary File S3. Dynamic visualization of the spatio-temporal reconstruction of the torquatus group origin and diffusion.